

Simple Three-Integral Scale-Free Galaxy Models

N.W. Evans,¹ R.M. Häfner¹ and P.T. de Zeeuw²

¹*Theoretical Physics, Department of Physics, 1 Keble Road, Oxford, OX1 3NP*

²*Sterrewacht Leiden, Postbus 9513, 2300 RA Leiden, The Netherlands*

ABSTRACT

The Jeans equations give the second moments or stresses required to support a stellar population against the gravity field. A general solution of the Jeans equations for arbitrary axisymmetric scale-free densities in flattened scale-free potentials is given. A two-parameter subset of the solution for the second moments for the self-consistent density of the power-law models, which have exactly spheroidal equipotentials, is examined in detail. In the spherical limit, the potential of these models reduces to that of the singular power-law spheres. We build the physical three-integral distribution functions that correspond to the flattened stellar components.

Next, we attack the problem of finding distribution functions associated with the Jeans solutions in flattened scale-free potentials. The third or partial integral introduced by de Zeeuw, Evans & Schwarzschild for Binney’s model is generalised to thin and near-thin orbits moving in arbitrary axisymmetric scale-free potentials. The partial integral is a modification of the total angular momentum. For the self-consistent power-law models, we show how this enables the construction of simple three-integral distribution functions. The connexion between these approximate distribution functions and the Jeans solutions is discussed in some detail.

Key words: celestial mechanics, stellar dynamics – galaxies: kinematics and dynamics – galaxies: structure

1 1 INTRODUCTION

Evidence both from hydrodynamical modelling of ellipticals (e.g., Binney, Davies & Illingworth 1990; van der Marel 1991) and the kinematics of the stellar halo of the Milky Way (e.g., Norris 1986; Morrison, Flynn & Freeman 1990) indicates that the phase space distribution functions (DFs) of elliptical galaxies and the haloes of spiral galaxies depend on three isolating integrals of motion.

General flattened potentials support fewer than three global isolating integrals. In triaxial systems, only the energy E is globally conserved. In axisymmetric potentials, the angular momentum component parallel to the symmetry axis L_z is also an invariant. Nonetheless, most stars do admit a third integral of motion that is a generalisation of the total angular momentum L (c.f., Saaf 1968; Innanen & Papp 1977; Lupton & Gunn 1987). The existence of chaotic trajectories prevents the extension of an analytic third integral to all the orbits. So, building three-integral DFs is often difficult in axisymmetric potentials. The problem is still more severe for triaxial systems (Schwarzschild 1979).

The natural shape of ellipticals and the haloes of spiral galaxies may well be triaxial. Nonetheless, it is still both useful and realistic to consider the somewhat simpler problem of how to construct three-integral axisymmetric stellar systems. Recently, de Zeeuw, Evans & Schwarzschild (1996, hereafter ZES) showed how to find a third, partial, integral of good accuracy for thin and near-thin tubes for oblate

scale-free potentials with flat rotation curves. They used the partial integral to build three-integral DFs and identified a class of physical solutions to the Jeans equations. The aim of this paper is to extend their methods and results to arbitrary axisymmetric scale-free potentials, with particular emphasis on the models with spheroidal equipotentials known as the power-law models (Evans 1994, hereafter E94).

The paper is arranged as follows. In Section 2, the Jeans approach is applied to yield the complete solution for the stresses or second order velocity moments that can support flattened populations of stars in scale-free potentials. A particularly simple two-parameter solution is identified for the self-consistent power-law models. Section 3 investigates the spherical limit. New families of three-integral DFs are presented and used to isolate the Jeans solutions of physical interest. With the insight gained from this simpler problem, we begin the harder job of constructing three-integral DFs for flattened scale-free potentials in Section 4. The third or partial integral introduced by ZES for the scale-free logarithmic potential (e.g., Binney & Tremaine 1987; see also Richstone 1980) is generalised to arbitrary axisymmetric scale-free potentials. We show by detailed numerical orbit integrations that it is a good integral for the thin and near-thin tube orbits, although it is not so well-conserved for fat tube orbits. Three integral DFs are then built in Section 5 and shown to correspond to a subset of the earlier Jeans solutions.

2 2 THE JEANS APPROACH

In this section, we use standard spherical coordinates (r, θ, ϕ) , with θ measured from the axis of symmetry and ϕ the azimuthal angle.

2.1 2.1 Scale-free potentials and densities

Scale-free axisymmetric potentials have the form

$$\Phi = -\frac{v_0^2}{\beta r^\beta g^{\beta/2}(\theta)}, \quad (2.1)$$

where $g(\theta)$ is an arbitrary function that describes the shape of the equipotentials. The circular velocity v_{circ} in the equatorial plane varies like $r^{-\beta/2}$. So, models with $\beta < 0$ have rising rotation curves, whereas models with $\beta > 0$ have falling rotation curves. When $\beta = 0$, the scale-free power-law potential becomes logarithmic, and we recover the special case already studied by ZES. The relevant range of β is from 1 corresponding to the outer Keplerian envelopes of star clusters to -2 corresponding to the shallow cusps of boxy ellipticals. Henceforth, we use units in which the velocity scale v_0 is unity.

It is often useful to consider tracer populations of stars moving in an external gravity field rather than the self-consistent stellar density generated by Poisson's equation. So, let us take the density to have the general scale-free form:

$$\rho = \frac{h(\theta)}{r^\gamma g^{2+\beta/2}(\theta)}. \quad (2.2)$$

Here, γ is a constant, which prescribes the radial fall-off of the density, while $h(\theta)$ is an arbitrary function. Both $g(\theta)$ and $h(\theta)$ are symmetric with respect to the equatorial plane, i.e., $g(\pi - \theta) = g(\theta)$ and $h(\pi - \theta) = h(\theta)$. When ρ is the self-consistent density, then $\gamma = 2 + \beta$ and $h(\theta)$ and $g(\theta)$ are related by ($4\pi G = 1$)

$$h(\theta) = (1 - \beta)g^2(\theta) + \frac{1}{2}g(\theta)g'(\theta)\cot\theta + \frac{1}{2}g(\theta)g''(\theta) - \frac{1}{2}g'(\theta)g'(\theta)(1 + \frac{1}{2}\beta). \quad (2.3)$$

When $\gamma \neq 2 + \beta$, the density (2.2) is greater than the density associated with the potential (2.1) either at large radii ($\gamma < 2 + \beta$) or at small radii ($\gamma > 2 + \beta$). However, we are often interested in the dynamics in particular régimes – such as the outer reaches or the cusp – and so this is not a grave drawback, provided the difficulty occurs outside the régime under scrutiny.

One pleasing choice for the arbitrary function $g(\theta)$ is

$$g(\theta) = \sin^2\theta + \frac{\cos^2\theta}{q^2}, \quad (2.4)$$

so that the equipotentials are similar concentric spheroids with axis ratio q . These are recognised as the power-law models introduced in E94. The associated self-consistent density is of the form (2.2), with

$$h(\theta) = Q\{(1 - \beta q^2)\sin^2\theta + [2 - Q(1 + \beta)]\cos^2\theta\}, \quad (2.5)$$

with $Q = q^{-2}$. In the spherical limit, $q = Q = 1$ and so $h(\theta) = 1 - \beta$.

2.2 2.2 General solution of the Jeans equations

The potential (2.1) and density (2.2) have the felicitous attribute of scale-freeness. Their properties at radius $r' = kr$ are just a magnification of those at radius r . Scale-free density distributions may have DFs that are not scale-free. For example, scale-free spheres can possess DFs built according to the instructions provided by Osipkov (1979) and Merritt (1985). These have an anisotropy radius, at which the properties of the velocity dispersion tensor change. However, let us assume that the associated DFs are also scale-free (e.g., Richstone 1980; White 1985; ZES), then the stresses have the following form:

$$\begin{aligned} \rho\langle v_r^2 \rangle &= \frac{F_1(\theta)}{r^{\beta+\gamma}g^{2+\beta}(\theta)}, & \rho\langle v_r v_\theta \rangle &= \frac{F_2(\theta)}{r^{\beta+\gamma}g^{2+\beta}(\theta)}, \\ \rho\langle v_\theta^2 \rangle &= \frac{F_3(\theta)}{r^{\beta+\gamma}g^{2+\beta}(\theta)}, & \rho\langle v_\phi^2 \rangle &= \frac{F_4(\theta)}{r^{\beta+\gamma}g^{2+\beta}(\theta)}, \end{aligned} \quad (2.6)$$

where F_1, F_2, F_3 , and F_4 are functions of θ , fulfilling the following conditions

$$\begin{aligned} F_1(\pi - \theta) &= F_1(\theta), & F_3(\pi - \theta) &= F_3(\theta), \\ F_2(\pi - \theta) &= -F_2(\theta), & F_4(\pi - \theta) &= F_4(\theta). \end{aligned} \quad (2.7)$$

As discussed in ZES, these constraints guarantee that the stresses are symmetric with respect to the equatorial plane. Substitution of the Ansatz (2.6) into the Jeans equations (ZES, equation 2.4) reduces them to two coupled first-order ordinary differential equations:

$$\begin{aligned} F_2'(\theta) + \left[\cot\theta - \frac{(2 + \beta)g'(\theta)}{g(\theta)} \right] F_2(\theta) \\ + (2 - \beta - \gamma)F_1(\theta) - F_3(\theta) - F_4(\theta) = -h(\theta), \end{aligned} \quad (2.8a)$$

$$\begin{aligned} F_3'(\theta) + \left[\cot\theta - \frac{(2 + \beta)g'(\theta)}{g(\theta)} \right] F_3(\theta) \\ + (3 - \beta - \gamma)F_2(\theta) - F_4(\theta)\cot\theta = -\frac{h(\theta)g'(\theta)}{2g(\theta)}. \end{aligned} \quad (2.8b)$$

The four functions $F_1(\theta), \dots, F_4(\theta)$ are therefore subject to the above two restrictions. We are at liberty to pick two of the functions arbitrarily and solve (2.8) for the other two. We choose to prescribe $F_1(\theta)$ and $F_2(\theta)$. Proceeding as in ZES, we use equation (2.8a) to eliminate $F_4(\theta)$ from (2.8b). It is straightforward to integrate the resulting first order differential equation for F_3 and then to substitute the result in (2.8a) to obtain F_4 . We find:

$$F_3(\theta) = I(\theta) + J(\theta) + F_2(\theta)\cot\theta, \quad (2.9a)$$

$$\begin{aligned} F_4(\theta) &= h(\theta) - I(\theta) - J(\theta) \\ &\quad - (\beta + \gamma - 2)F_1(\theta) + g^{\beta+2}(\theta) \frac{d}{d\theta} \left[\frac{F_2(\theta)}{g^{\beta+2}(\theta)} \right], \end{aligned} \quad (2.9b)$$

with

$$I(\theta) = \frac{g^{\beta+2}(\theta)}{\sin^2\theta} \int_0^\theta d\theta \frac{\sin^2\theta}{g^{\beta+2}(\theta)} \left[\cot\theta - \frac{g'(\theta)}{2g(\theta)} \right] h(\theta), \quad (2.10)$$

and

$$J(\theta) = \frac{(\beta + \gamma - 2)g^{\beta+2}(\theta)}{\sin^2 \theta} \times \int_0^\theta d\theta \frac{\sin^2 \theta}{g^{\beta+2}(\theta)} [F_2(\theta) - F_1(\theta) \cot \theta]. \quad (2.11)$$

Hence, the stresses can be found by evaluation of the integrals for $I(\theta)$ and $J(\theta)$. It follows that

$$F_3(0) = F_4(0) = \frac{1}{2}h(0) - \frac{1}{2}(\beta + \gamma - 2)F_1(0). \quad (2.12)$$

This means that $\langle v_\theta^2 \rangle = \langle v_\phi^2 \rangle$ on the minor axis, as is required by elementary symmetry arguments (e.g., Bacon 1985). Let us note that the case $\gamma + \beta = 2$ is special, as then the integral $J(\theta)$ drops out of the solution (2.9). The only self-consistent model ($\gamma = 2 + \beta$) for which this happens has $\beta = 0$ and $\gamma = 2$. This completes our derivation of the general solution of the Jeans equations for galaxies with scale-free potentials (2.1) and scale-free densities of the form (2.2). The condition that the principal components of the stress tensor are positive definite is given in section 2.4 of ZES.

2.3 The two-integral limit: $f = f(E, L_z^2)$

Let us consider briefly the special case corresponding to a two-integral DF $f = f(E, L_z^2)$, in which the stellar velocities have no preferred direction in the meridional plane, i.e., $\langle v_r^2 \rangle \equiv \langle v_\theta^2 \rangle$ and $\langle v_r v_\theta \rangle \equiv 0$. It is straightforward to find the associated stresses solution by taking

$$F_1(\theta) \equiv F_3(\theta), \quad F_2(\theta) \equiv 0. \quad (2.13)$$

Substitution of (2.13) in equations (2.9a) and (2.11) results in a Volterra integral equation for F_1 which is solved to give

$$F_1(\theta) = \frac{g^{\beta+2}(\theta)}{\sin^{\beta+\gamma}\theta} \int_0^\theta d\theta \frac{\sin^{\beta+\gamma}\theta}{g^{\beta+2}(\theta)} \left[\cot \theta - \frac{g'(\theta)}{2g(\theta)} \right] h(\theta). \quad (2.14)$$

Substitution of this expression in equation (2.9b) provides $F_4(\theta)$ as:

$$F_4(\theta) = h(\theta) + (1 - \beta - \gamma)F_1(\theta). \quad (2.15)$$

These results can be checked using Hunter's (1977) solution of the Jeans equations for general $f(E, L_z^2)$ models.

2.4 A two-parameter solution for the self-consistent power-law models

Let us now specialise to the specific case of the self-consistent power-law models. We take $g(\theta)$ and $h(\theta)$ as given in (2.4) and (2.5), while $\gamma = 2 + \beta$. Evans & de Zeeuw (1994) showed that when the stresses have the simple form

$$\rho \langle v_j^2 \rangle = \frac{a_j R^2 + b_j R z + c_j z^2}{(R^2 + z^2/q^2)^{2+\beta}}, \quad (2.16)$$

then the line-of-sight projected second moments – such as the dispersions in the radial velocities and the proper motions – can be explicitly evaluated as elementary functions. As a matter of choice, we elect to study the subset of the general solution (2.9) that possesses this fetching property. This implies choosing

$$\begin{aligned} F_1(\theta) &= I(\theta) + J(\theta) + H_1 + H_2 g(\theta) \sin^2 \theta, \\ F_2(\theta) &= H_2 g(\theta) \sin \theta \cos \theta. \end{aligned} \quad (2.17)$$

Table 1. Coefficients for the Jeans solution (2.20), with $Q = q^{-2}$.

A_1	$H_1(1 + \beta - \beta q^2) + H_2(1 + \beta) + \frac{1}{2}(1 - \beta)$
C_1	$QH_2(1 + \beta) - \beta H_1 + \frac{1}{2}Q[2 - Q(1 + \beta)]$
B_2	$H_1(1 + \beta)$
A_3	$\frac{1}{2}(1 - \beta) - \beta q^2 H_1$
C_3	$H_1 + \frac{1}{2}Q(2 - Q(1 + \beta))$
A_4	$Q(1 + \beta) - \frac{1}{2}(1 + 3\beta) - H_2(1 + \beta)(1 + 2\beta) + \beta H_1[q^2(1 + 2\beta) - 2(1 + \beta)]$
C_4	$QH_2(1 + \beta) - \beta H_1 + \frac{1}{2}Q[2 - Q(1 + \beta)]$

Here, $I(\theta) + J(\theta)$ is

$$\begin{aligned} I(\theta) + J(\theta) &= \frac{1}{2} \frac{1 - \beta}{1 + \beta} \sin^2 \theta - \frac{\beta}{1 + \beta} H_1 q^2 g(\theta) \\ &\quad + \frac{1}{2} \frac{Q[2 - Q(1 + \beta)]}{1 + \beta} \cos^2 \theta, \end{aligned} \quad (2.18)$$

while H_1 and H_2 are constants. Of course, this is a very restricted subset of the general solution (2.9) – instead of two free functions $F_1(\theta)$ and $F_2(\theta)$, we have merely two free parameters H_1 and H_2 . They have a simple physical interpretation. $H_1 = 0$ means that the velocity ellipsoids are aligned with the cylindrical coordinate system, while $H_2 = 0$ means that they are aligned with the spherical coordinate system.

Substitution of the choice (2.17) in the general solution (2.9) yields

$$\begin{aligned} F_3(\theta) &= I(\theta) + J(\theta) + H_2 g(\theta) \cos^2 \theta, \\ F_4(\theta) &= h(\theta) - I(\theta) - J(\theta) - 2\beta F_1(\theta) \\ &\quad + H_2 [Q \cos^2 \theta - \sin^2 \theta - 2\beta(1 - Q) \sin^2 \theta \cos^2 \theta]. \end{aligned} \quad (2.19)$$

This seems complicated, but when we write the Jeans solution out explicitly in cylindrical coordinates, it is simply:

$$\begin{aligned} \rho \langle v_R^2 \rangle &= \frac{A_1 R^2 + C_1 z^2}{(1 + \beta)(R^2 + z^2/q^2)^{2+\beta}}, \\ \rho \langle v_R v_z \rangle &= \frac{B_2 R z}{(1 + \beta)(R^2 + z^2/q^2)^{2+\beta}}, \\ \rho \langle v_z^2 \rangle &= \frac{A_3 R^2 + C_3 z^2}{(1 + \beta)(R^2 + z^2/q^2)^{2+\beta}}, \\ \rho \langle v_\phi^2 \rangle &= \frac{A_4 R^2 + C_4 z^2}{(1 + \beta)(R^2 + z^2/q^2)^{2+\beta}}, \end{aligned} \quad (2.20)$$

where the relationships between the coefficients A_j, B_j, C_j and our two anisotropy parameters H_1 and H_2 are given in Table 1. Lastly, let us remark that the two-parameter Jeans solution (2.20) admits an extension to cored models that is discussed in Appendix A.

2.5 Limits on the two-parameter solution

The principal stresses $\rho \langle v_\lambda^2 \rangle$ and $\rho \langle v_\nu^2 \rangle$ of the two-parameter Jeans solution for the power-law models are

$$\rho \langle v_\lambda^2 \rangle = \frac{F_-(\theta)}{r^{\beta+\gamma} g^2(\theta)}, \quad \rho \langle v_\nu^2 \rangle = \frac{F_+(\theta)}{r^{\beta+\gamma} g^2(\theta)}, \quad (2.21)$$

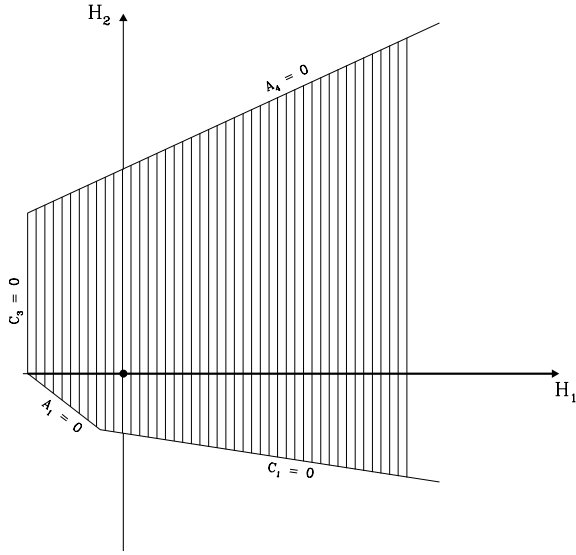


Figure 1. The (H_1, H_2) -plane of two-parameter anisotropic solutions of the Jeans equations for the self-consistent power-law models with $\beta = -0.25$ and $q = 0.87$. The hatched area corresponds to the solutions of the Jeans equations with non-negative stresses $\rho\langle v_R^2 \rangle$, $\rho\langle v_z^2 \rangle$, and $\rho\langle v_\phi^2 \rangle$. The requirement that the principal components of the stress tensor $\rho\langle v_\lambda^2 \rangle$ and $\rho\langle v_\nu^2 \rangle$ be positive definite leads to two further small areas in the bottom left quadrant being deleted. The line $H_1 = 0$ gives the cylindrically aligned models, while the line $H_2 = 0$ gives spherically aligned models.

with

$$F_\pm(\theta) = I(\theta) + J(\theta) + \frac{1}{2}H_1 + \frac{1}{2}H_2 g(\theta) \pm \sqrt{H_1^2 - 2H_1H_2 g(\theta) \cos 2\theta + H_2^2 g^2(\theta)}. \quad (2.22)$$

The tilt angle Θ of the velocity ellipsoid in the meridional plane is the misalignment with respect to the spherical polar coordinate surfaces. It is:

$$\tan 2\Theta = \frac{2F_2}{F_1 - F_3} = \frac{H_2 g(\theta) \sin 2\theta}{H_1 - H_2 g(\theta) \cos 2\theta}. \quad (2.23)$$

Necessary (but *not* sufficient) requirements for positive stresses are that $\rho\langle v_R^2 \rangle$, $\rho\langle v_z^2 \rangle$ and $\rho\langle v_\phi^2 \rangle$ are non-negative. This implies the following conditions on H_1 and H_2 :

$$\begin{aligned} -\frac{1}{2}Q[2 - Q(1 + \beta)] &\leq H_1, \\ \frac{1}{2}Q(1 + \beta) - 1 &\leq (1 + \beta)H_2 - \beta q^2 H_1, \\ -\frac{1}{2}(1 - \beta) &\leq (1 + \beta)H_2 \\ &+ (1 + \beta - \beta q^2)H_1, \\ Q(1 + \beta) - \frac{1}{2}(1 + 3\beta) &\geq H_2(1 + \beta)(1 + 2\beta) \\ &- \beta[q^2(1 + 2\beta) - 2 - 2\beta]H_1. \end{aligned} \quad (2.24)$$

These define a hatched region in the (H_1, H_2) -plane illustrated in Figs. 1 and 2 for models with rising and falling rotation curves respectively. Note that when $\beta < 0$, the hatched region extends to infinity along the $H_2 = 0$ axis. When $\beta > 0$, there exists a limiting value of H_1 , namely $Q(1 - 2\beta + q^2)/(4\beta)$, beyond which the Jeans solutions become negative. The case $\beta = 0$ discussed in ZES is intermediate, in the sense that the upper and lower boundaries of

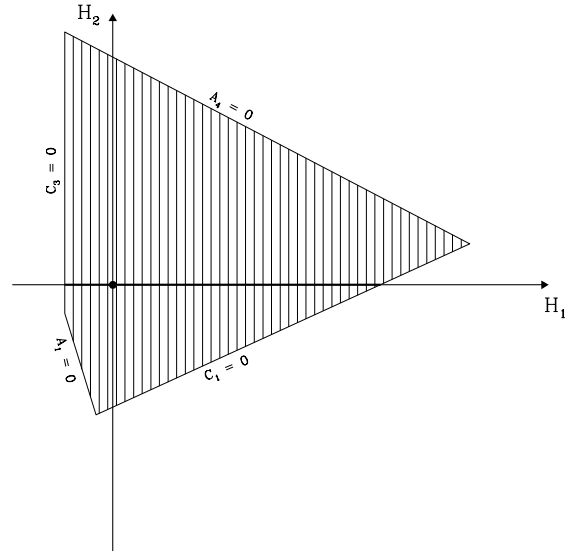


Figure 2. As Fig. 1, but for $\beta = 0.18$ and $q = 0.9$. The hatched area now closes, and it is not possible to find Jeans solutions with arbitrarily large radial anisotropy. Note that the largest value of H_1 consistent with positive stresses is $Q(1 - 2\beta + q^2)/(4\beta)$. This occurs when the lines $C_1 = 0$ and $A_4 = 0$ intersect. Adding in the additional condition that the solution is spherically aligned ($H_2 = 0$) gives the more stringent condition $\beta H_1 < Q(1 - \frac{1}{2}Q(1 + \beta))$.

the hatched region are exactly horizontal.

Necessary *and* sufficient conditions for positive stresses are that the principal components $\rho\langle v_\lambda^2 \rangle$ and $\rho\langle v_\nu^2 \rangle$ (or, equivalently, their sum and product) are non-negative. This problem can be solved using the same methods as in section 2.7 of ZES. The additional regions that must be discarded from Figs. 1 and 2 are those simultaneously satisfying the four inequalities written out in detail in Appendix B. In fact, this results in the removal of only two small areas near the two corners of the hatched region that lie in the third quadrant of Figs. 1 and 2, respectively. They lie away from the spherically aligned Jeans solutions ($H_2 = 0$), for which we will construct approximate DFs in Section 5. As these additional, tiny forbidden areas are not particularly important for the purposes of this paper, we have not complicated Figs. 1 and 2 by marking them.

The position of the two-integral solution (2.13) is marked in Figs. 1 and 2 – it lies at the origin in the (H_1, H_2) -plane. As shown in E94, it is generated by a positive definite DF provided the flattening satisfies $q^2 \geq \frac{1}{2}(1 + \beta)$. Note that this constraint can also be deduced from the first equation of (2.24) on putting $H_1 = 0$. It is clear from Figs. 1 and 2 that the set of Jeans solutions for the self-consistent power-law models is large. The rest of the paper addresses the question: which solutions are physically relevant and correspond to positive DFs?

3 SPHERICAL POTENTIALS

Now let us suppose the potential is exactly spherical. The beauty of this assumption is that it enables the construction

of flattened components with simple three-integral DFs and triaxial kinematics. This is because the total angular momentum L is an exact integral of motion in a spherical potential well, in addition to the angular momentum component about the symmetry axis L_z . As first realised by White (1985), such DFs give realistic descriptions of the kinematics of tracer populations of stars in the outer reaches of galaxies.

3.1 General Jeans Solutions and Distribution Functions

If the gravity field is spherically symmetric, then $g(\theta) \equiv 1$ and (2.1) reduces to the potential of the singular power-law spheres (E94). The work in the previous section allows us to deduce the general solution for the stresses associated with a flattened density $\rho = r^{-\gamma} h(\theta)$. It is of the form (2.6) with $g(\theta) \equiv 1$. The functions $F_1(\theta)$ and $F_2(\theta)$ are arbitrary, while $F_3(\theta)$ and $F_4(\theta)$ follow from (2.9) with $g(\theta) \equiv 1$. However, in a spherical potential, we must have $\langle v_r v_\theta \rangle \equiv 0$ (see e.g., ZES). So, only the solutions with $F_2(\theta) \equiv 0$ are physical! They have the form

$$\begin{aligned} F_3(\theta) &= I(\theta) + J(\theta), \\ F_4(\theta) &= h(\theta) - I(\theta) - J(\theta) - (\beta + \gamma - 2)F_1(\theta), \end{aligned} \quad (3.1)$$

and

$$I(\theta) = \frac{1}{\sin^2 \theta} \int_0^\theta h(\theta) \sin \theta \cos \theta d\theta, \quad (3.2)$$

$$J(\theta) = \frac{(2 - \beta - \gamma)}{\sin^2 \theta} \int_0^\theta F_1(\theta) \sin \theta \cos \theta d\theta.$$

Here, $F_1(\theta)$ – or the angular variation of the radial velocity dispersion – is arbitrary. Once it and $h(\theta)$ have been chosen, the other second moments are fixed. When $\beta + \gamma = 3$, we have $\langle v^2 \rangle \equiv \langle v_r^2 \rangle + \langle v_\theta^2 \rangle + \langle v_\phi^2 \rangle \equiv r^{-\beta}$. A special case of this rule was noted earlier by Maoz & Bekenstein (1990), who pointed out that if the velocity dispersion is independent of both r and θ , then the potential is logarithmic ($\beta = 0$) and the density profile must fall like r^{-3} (i.e., $\gamma = 3$).

Now $h(\theta)$ and $F_1(\theta)$ are even functions symmetric about $\theta = \pi/2$. They may be expanded as a series of even powers of $\sin \theta$ (see e.g., Mathews & Walker 1964; ZES):

$$h(\theta) = \sum_{n=0}^{\infty} a_n \sin^{2n} \theta, \quad F_1(\theta) = \sum_{n=0}^{\infty} b_n \sin^{2n} \theta. \quad (3.3)$$

Our aim is to find DFs generating the Jeans solution (3.1) corresponding to each pair $h(\theta), F_1(\theta)$. First, we note that the stellar density law $r^{-\gamma} \sin^{2n} \theta$ can be reproduced by non-negative DFs of the form

$$f_{m,n}(E, L^2, L_z^2) = \eta_{m,n} L^{2m} L_z^{2n} |E|^\alpha, \quad (3.4)$$

where

$$\alpha = \frac{(2 - \beta)(m + n)}{\beta} + \frac{\gamma}{\beta} - \frac{3}{2}. \quad (3.5)$$

and $m + n > -1$, $2n > -1$ and

$$\gamma + 2m + 2n > \begin{cases} 0, & \text{if } \beta < 0, \\ \beta(m + n + \frac{1}{2}), & \text{if } \beta > 0. \end{cases} \quad (3.6)$$

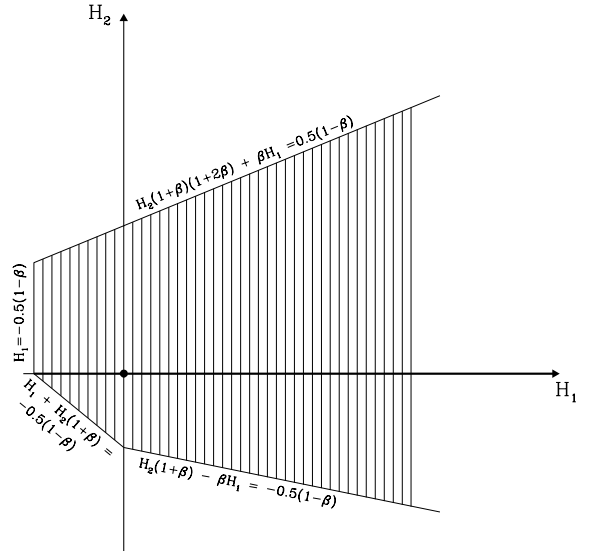


Figure 3. The (H_1, H_2) -plane of two-parameter anisotropic solutions of the Jeans equations for the singular self-consistent power-law spheres with rising rotation laws ($\beta < 0$). The hatched region indicates the area with everywhere positive stresses. The filled circle corresponds to the isotropic model ($H_1 = 0, H_2 = 0$). The physical solutions are those that are spherically aligned – these lie on the thickened, bold line $H_2 = 0$, subject only to the condition that $H_1 > -\frac{1}{2}(1 - \beta)$.

Note that we have written m and n so that our notation is consistent with White (1985) and ZES, but m and n are not necessarily integers. The normalization constant $\eta_{m,n}$ is

$$\eta_{m,n} = \frac{|\beta|^{2m/\beta + 2n/\beta + \gamma/\beta}}{\sqrt{\pi} 2^{m+n+3/2} \Gamma(m+n+1) B(1/2, n+1/2)} \times \begin{cases} \frac{\Gamma(-\alpha)}{\Gamma(-\gamma/\beta - 2m/\beta - 2n/\beta)}, & \text{if } \beta < 0, \\ \frac{\Gamma(\gamma/\beta + 2m/\beta + 2n/\beta + 1)}{\Gamma(\alpha + 1)}, & \text{if } \beta > 0. \end{cases} \quad (3.7)$$

Here, $B(x, y) = \Gamma(x)\Gamma(y)/\Gamma(x+y)$ is the beta function.

By integrating over all velocity space, the corresponding stresses are

$$\begin{aligned} \rho \langle v_r^2 \rangle &= \frac{1}{2m + 2n + \beta + \gamma} \frac{\sin^{2n} \theta}{r^{\beta + \gamma}}, \\ \rho \langle v_\theta^2 \rangle &= \frac{m + n + 1}{n + 1} \rho \langle v_r^2 \rangle, \\ \rho \langle v_\phi^2 \rangle &= (2n + 1) \rho \langle v_\theta^2 \rangle. \end{aligned} \quad (3.8)$$

The angular dependence of the density is independent of m for fixed γ and n . The same is true of the stresses. However, the anisotropy ratios $\langle v_\theta^2 \rangle / \langle v_r^2 \rangle$ and $\langle v_\phi^2 \rangle / \langle v_r^2 \rangle$ do vary with m . Whenever $\gamma + \beta = 3$, then $\langle v_r^2 \rangle + \langle v_\theta^2 \rangle + \langle v_\phi^2 \rangle = v_{\text{circ}}^2$. In the limit $\beta \rightarrow 0$, the components reduce to those studied in White (1985), Gerhard (1991) and ZES. The components for $\beta > 0$ have previously been discussed by Kulessa & Lynden-Bell (1992) and de Bruijne, van der Marel & de Zeeuw (1996). Using the method of linear superposition of

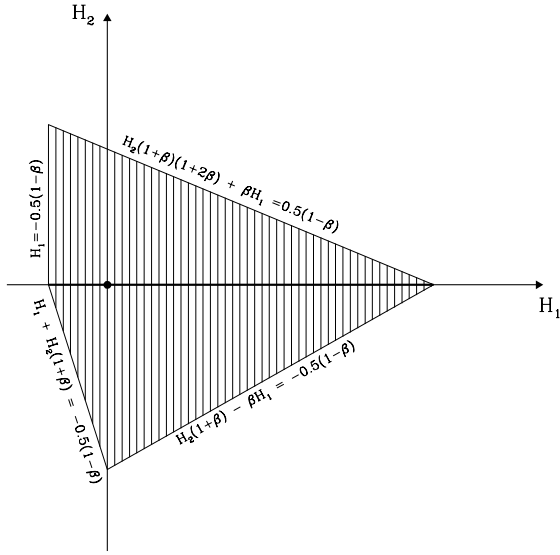


Figure 4. As Fig. 3, but for the self-consistent power-law spheres with falling rotation laws ($\beta > 0$). Note that the physical solutions (corresponding to the thickened, bold line) are more restricted than in Fig. 3. They encompass those parts of the line $H_2 = 0$, subject to $-\frac{1}{2}(1-\beta) \leq H_1 < \frac{1}{2}(1-\beta)/\beta$.

the components (3.4), the general solution of the Boltzmann equation becomes

$$f(E, L^2, L_z^2) = \sum_{m,n} A_{m,n} f_{m,n}. \quad (3.9)$$

Here, the $A_{m,n}$ are constants specifying the fraction contributed by each component. To build DFs that recover the angular variation $h(\theta)$ of the density and $F_1(\theta)$ of the radial velocity dispersion of our Jeans solution, we must insist that:

$$\sum_{m=0}^{\infty} A_{m,n} = a_n, \quad \sum_{m=0}^{\infty} \frac{A_{m,n}}{2m+2n+\beta+\gamma} = b_n, \quad (3.10)$$

for $n = 0, 1, 2, \dots$. There are many more unknowns $A_{m,n}$ than constraints a_n, b_n . So, there are many ways to define three-integral DFs that reproduce the required density and velocity dispersions. For specific choices of $h(\theta)$, examples of such DFs are given in Kulessa & Lynden-Bell (1992) and de Bruijne, van der Marel & de Zeeuw (1996).

As an aside, we remark that it is possible to generalise (3.4) to produce triaxial stellar distributions with triaxial kinematics in spherical potentials. In view of its ready application to the kinematics of the stellar halo of the Milky Way Galaxy, this development is discussed in more detail in Appendix C.

3.2 A one-parameter solution for self-consistent spherical models

Let us now consider the limiting behavior of the two-parameter Jeans solutions for the self-consistent power-law spheres. Not just the potential, but also the density, is now

spherical. Using $h(\theta) \equiv 1 - \beta$, $g(\theta) \equiv 1$ and $\gamma = 2 + \beta$, we find from equations (2.17) that

$$\begin{aligned} F_1(\theta) &= \frac{1-\beta+2H_1}{2(1+\beta)} + H_2 \sin^2 \theta, \\ F_2(\theta) &= H_2 \sin \theta \cos \theta, \\ F_3(\theta) &= \frac{1-\beta-2\beta H_1}{2(1+\beta)} + H_2 \cos^2 \theta, \\ F_4(\theta) &= \frac{1-\beta-2\beta H_1}{2(1+\beta)} + H_2 [\cos^2 \theta - \sin^2 \theta (1+2\beta)]. \end{aligned} \quad (3.11)$$

These anisotropic stresses for the self-consistent, singular power-law spheres are positive in the region in the (H_1, H_2) -plane defined by (cf. eq. [2.24])

$$\begin{aligned} -\frac{1}{2}(1-\beta) &\leq H_1, \\ -\frac{1}{2}(1-\beta) &\leq H_2(1+\beta) - \beta H_1, \\ -\frac{1}{2}(1-\beta) &\leq H_2(1+\beta) + H_1, \\ \frac{1}{2}(1-\beta) &\geq H_2(1+\beta)(1+2\beta) + \beta H_1, \end{aligned} \quad (3.12)$$

which is illustrated in Figs. 3 and 4 for power-law spheres with rising ($\beta < 0$) and falling ($\beta > 0$) rotation laws. As we have seen, all physical solutions must have $F_2 \equiv 0$ because of the properties of individual orbits. On requiring that $H_2 = 0$, we are left with a one-parameter solution

$$\begin{aligned} F_1(\theta) &= \frac{1-\beta+2H_1}{2(1+\beta)}, \\ F_3(\theta) = F_4(\theta) &= \frac{1-\beta-2\beta H_1}{2(1+\beta)}, \end{aligned} \quad (3.13)$$

which is indicated as the thick solid line in Figs. 3 and 4. It follows from the derivation in Section 3.1 that each of these Jeans solutions corresponds to a DF of the general form (3.9) with $n = 0$, so that

$$f(E, L^2) = \sum_{m=0}^{\infty} A_{m,0} \eta_{m,0} L^{2m} |E|^{2(m+1)/\beta - m - 1/2}, \quad (3.14)$$

with $\eta_{m,0}$ given in equation (3.7). The coefficients are subject to the constraints

$$\sum_{m=0}^{\infty} A_{m,0} = 1 - \beta, \quad \sum_{m=0}^{\infty} \frac{A_{m,0}}{m+\beta+1} = \frac{1-\beta+2H_1}{1+\beta}. \quad (3.15)$$

Again, many DFs are possible. The simplest is obtained by taking only one component in the series (3.14):

$$f(E, L^2) = \eta_{m,0} L^{2m} |E|^{2(m+1)/\beta - m - 1/2}, \quad (3.16)$$

with

$$m = \frac{-2H_1(\beta+1)}{1+2H_1-\beta}. \quad (3.17)$$

Of course, H_1 is a measure of the anisotropy of the model. $H_1 = -\frac{1}{2}(1-\beta)$ corresponds to the circular orbit model (no radial velocity dispersion) and $H_1 = 0$ to the isotropic model. When $\beta \leq 0$, then $H_1 \rightarrow \infty$ and the model approaches the radial orbit model. When $\beta > 0$, then the most radially distended model possible (see Fig. 4) has $H_1 = (1-\beta)/(2\beta)$. This corresponds to the critical value of $m = -1$, for which (3.4) ceases to exist. The DF (3.16) is non-negative and so physical for each of these permitted values of H_1 .

Table 2. Accuracy of the partial integral I_3 for an E3 power-law model with a falling rotation curve ($\beta = 0.18, q = 0.9$). Meridional cross sections of the orbits are displayed in Fig. 5.

q	R_0	z_0	L_z	$I_{3,\max}$	$I_{3,\min}$	δI_3	L_{\max}^2	L_{\min}^2	δL^2
Thin tubes in E3 galaxies									
A 0.9	.5232	.2384	.541	.3678	.3677	.0001	.3677	.3534	.0143
B 0.9	.3794	.4268	.378	.3671	.3660	.0011	.3660	.3236	.0424
C 0.9	.1889	.5367	.182	.3657	.3630	.0027	.3630	.3004	.0626
D 0.9	.0472	.5667	.045	.3651	.3617	.0034	.3617	.2935	.0682
Fat tubes in E3 galaxies									
E 0.9	.4800	.4853	.378	.3499	.3208	.0291	.3484	.2889	.0595
F 0.9	.6600	.4529	.378	.2583	.2208	.0375	.2531	.2094	.0437
G 0.9	.8400	.2425	.378	.1666	.1555	.0111	.1650	.1539	.0111

Table 3. Accuracy of the partial integral I_3 for an E3 power-law model with a rising rotation curve ($\beta = -0.25, q = 0.87$).

q	R_0	z_0	L_z	$I_{3,\max}$	$I_{3,\min}$	δI_3	L_{\max}^2	L_{\min}^2	δL^2
Thin tubes in E3 galaxies									
A 0.87	.5852	.2573	.541	.3677	.3674	.0003	.3674	.3493	.0181
B 0.87	.4334	.4677	.378	.3653	.3628	.0025	.3627	.3094	.0533
C 0.87	.2220	.6003	.182	.3600	.3527	.0073	.3527	.2753	.0774
D 0.87	.0562	.6395	.045	.3566	.3477	.0089	.3477	.2640	.0837
Fat tubes in E3 galaxies									
E 0.87	.4800	.4961	.378	.3678	.3438	.0240	.3676	.2955	.0721
F 0.87	.6600	.4927	.378	.3037	.2444	.0593	.3010	.2225	.0785
G 0.87	.8400	.3423	.378	.2079	.1742	.0337	.2027	.1666	.0361

4 THE BOLTZMANN APPROACH

The Boltzmann approach emphasises the primacy of distribution functions (DFs). In this section, we investigate which of the two-parameter Jeans solutions can correspond to three-integral DFs for the flattened power-law potentials. To do this, we must first extend the theory of partial integrals introduced in ZES.

4.1 Classical and partial integrals

The collisionless Boltzmann equation for the DF f can be cast into the form

$$0 = v_r A + v_\theta B, \quad (4.1)$$

with

$$A = \frac{1}{2} r \frac{\partial f}{\partial r} + (v_\theta^2 + v_\phi^2 - r \frac{\partial \Phi}{\partial r}) \frac{\partial f}{\partial v_r^2} - v_\theta^2 \frac{\partial f}{\partial v_\theta^2} - v_\phi^2 \frac{\partial f}{\partial v_\phi^2}, \quad (4.2)$$

and

$$B = \frac{1}{2} \frac{\partial f}{\partial \theta} - \frac{\partial \Phi}{\partial \theta} \frac{\partial f}{\partial v_\theta^2} + v_\phi^2 \cot \theta \left(\frac{\partial f}{\partial v_\theta^2} - \frac{\partial f}{\partial v_\phi^2} \right). \quad (4.3)$$

Of course, any axisymmetric potential has two classical integrals, the energy $E = \Phi + \frac{1}{2}(v_r^2 + v_\theta^2 + v_\phi^2)$ and the z -component of the angular momentum $L_z = r v_\phi \sin \theta$. With the exception of special potentials possessing additional symmetries in phase space, axisymmetric potentials do not have exact, globally defined third integrals (e.g., Lynden-Bell 1962; de Zeeuw 1985; Evans 1990). This is awkward for

stellar dynamics, as the observational data require three-integral DFs. One way round this problem is suggested in ZES. We look for partial integrals which have good accuracy for some orbital families, rather than the global integrals which we know in general do not exist. ZES constructed such a partial integral for the thin and near-thin tubes in a scale-free model with a flat rotation curve (Binney's model). Here, our aim is to understand how this partial integral extends to the entire scale-free family.

In the spherical limit, the potential has an exact third integral, namely the total angular momentum $L^2 = r^2(v_\theta^2 + v_\phi^2)$. ZES introduced a modification

$$I_3 = L^2 i_3(\theta) = r^2(v_\theta^2 + v_\phi^2) i_3(\theta), \quad (4.4)$$

and showed that a suitable choice for Binney's model was $i_3(\theta) = \sin^2 \theta + Q \cos^2 \theta$. Inserting our ansatz I_3 into the Boltzmann equation (4.1), we find that

$$A = 0, \quad (4.5)$$

$$B = \frac{1}{2} r^2 i_3'(\theta) \left[v_\theta^2 + v_\phi^2 - \frac{1}{r^\beta} \frac{i_3(\theta) g'(\theta)}{i_3'(\theta) g^{1+\beta/2}(\theta)} \right].$$

The thin or near-thin tubes have the property that

$$v_\theta^2 + v_\phi^2 \approx -r \frac{\partial \Phi}{\partial r} = \frac{1}{r^\beta g^{\beta/2}(\theta)}, \quad (4.6)$$

is fulfilled. This essentially states that anywhere on a thin tube, v_r is much smaller than the other two components. This itself implies that, in the meridional plane, the thin tubes lie very nearly on circles. This is certainly a good

approximation in moderately flattened models (like E3). The partial integral therefore satisfies the collisionless Boltzmann equation if

$$\frac{1}{i_3} \frac{di_3}{d\theta} = \frac{1}{g} \frac{dg}{d\theta}. \quad (4.7)$$

Straightforward integration gives

$$i_3(\theta) = g(\theta), \quad (4.8)$$

and so the third integral is just

$$I_3 = r^2(v_\theta^2 + v_\phi^2)g(\theta). \quad (4.9)$$

This is exactly the same as deduced by ZES for the specific case of Binney's model. We emphasise, though, that the only assumption involved in deriving (4.8) is that of scale-freeness of the potential. The claim is that this is a good partial integral for thin and near-thin tubes in *any* galaxy with a scale-free potential.

4.2 Numerical integrations

The accuracy of the partial integral is now investigated by adaptive Runge-Kutta techniques for the specific cases of the self-consistent scale-free power-law galaxies (i.e., $g(\theta)$ is given by (2.4)). The results of such computations are listed in Tables 2 and 3, while Fig. 5 shows cross-sections of the orbits in the meridional plane. To ease comparison with the results of ZES, the energy surface is always normalised to

$$E = \frac{1}{2} \frac{\beta - 2}{\beta} \exp\left[\frac{\beta}{2 - \beta}\right], \quad \beta \neq 0. \quad (4.10)$$

This ensures that the limiting angular momentum of the circular orbit is $e^{-1/2}$. For the purposes of illustration, we concentrate on one model with falling rotation curve ($\beta = 0.18, q = 0.9, E = -5.5811$) and one model with rising rotation curve ($\beta = -0.25, q = 0.87, E = 4.0268$). The rationale behind the choices of the equipotential axis ratio q is that the galaxies have the same asymptotic ellipticity of E3 (using formula (2.9) of E94). The values of β are suggested by taking the means of the asymptotic logarithmic gradients of the rotation curves in the samples of Casertano & van Gorkom (1991). In Tables 2 and 3, the orbits are identified by their starting values R_0 and z_0 , with v_r and v_θ zero there. The maximum and minimum values of I_3 and L^2 are recorded, together with their fluctuation. Figure 5 shows cross-sections of the orbits for $\beta = 0.18$ (the diagram for $\beta = -0.25$ is very similar). The thin tubes are labelled A, B, C, and D. For all these thin tubes, the partial integral is well-conserved. The lower section of Tables 2 and 3 shows the results for thicker tube orbits. Now the variation in the partial integral is larger – but it is still more accurately conserved than the total angular momentum. The partial integral is not exact, even for the thin tubes. At any angular momentum L_z , there is a unique infinitesimally thin tube with energy (4.10). Fig. 6 shows the fluctuation in I_3 (expressed as a percentage) along the thin tubes for the three values $\beta = 0.18, 0.0$ and -0.25 . This illustrates graphically that the fluctuations in the partial integral are smaller for the models with falling rotation curves. Note that, even for the thin tubes, the partial integral is not exact.

Can the partial integral accurately distinguish between different orbital families or – equivalently – different tori

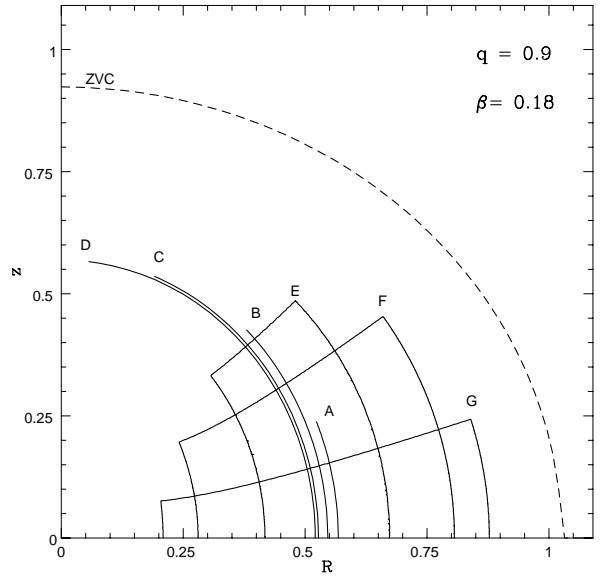


Figure 5. Cross sections of the orbits of Table 2 with a meridional plane (R, z) for the scale-free power-law potential $q = 0.9$ at energy $E = -5.5811$. The zero-velocity curve (for $L_z = 0$) is indicated by the ZVC. Orbits A - D are thin tubes. Orbits E - G are fat (or thick) tubes that fill the indicated areas. (Cross-sections of the orbits in Table 3 look very similar).

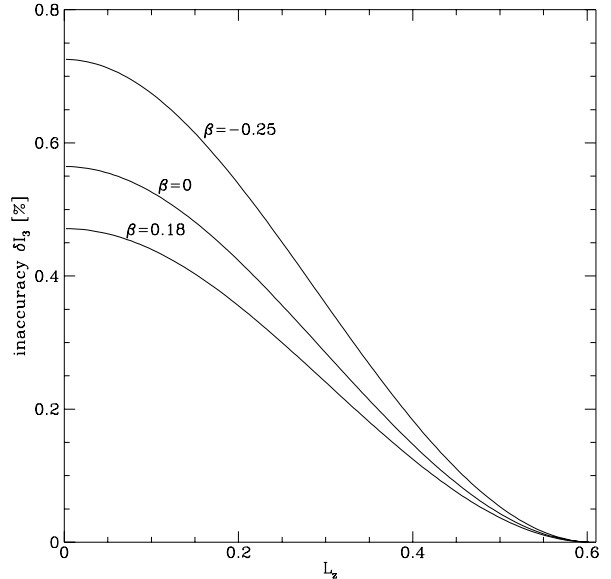


Figure 6. The fluctuation in the partial integral for the infinitesimally thin tubes (expressed as a percentage) is plotted against the angular momentum for three values of β . Even for the thin tubes, the partial integral is not exact, although it is very good. The diagram clearly illustrates that the partial integral worsens in accuracy as β diminishes. (All the models have $q = 0.9$).

in phase space? One way to establish this is to investigate the phase space structure using Poincaré surfaces of section (see e.g., Gutzwiller 1990). Fig. 7 shows surfaces of section for the model with a falling rotation curve ($\beta = 0.18, q =$

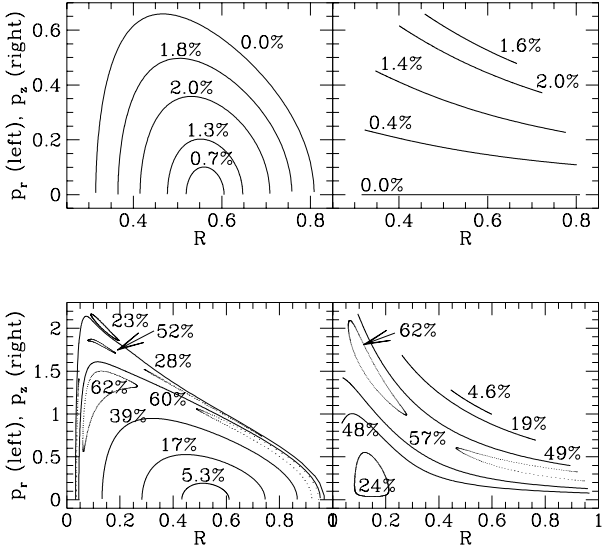


Figure 7. Poincaré surfaces of section for the model with $\beta = 0.18$ and $q = 0.9$. The energy hypersurface is normalised to $E = -5.5811$. The upper and lower panels show the the (R, p_R) and (R, p_z) cross-sections of the energy hypersurface at the equatorial plane for $L_z = 0.5$ and at $L_z = 0.1$ respectively. Each orbit is marked with the fluctuation in the partial integral represented as a percentage. At high L_z , the orbits are mainly thin and near-thin tubes. As is evident from the upper two panels, the partial integral is well-conserved by all the orbits. At low L_z , minor orbital families trapped around the 1 : 1 and 3 : 4 resonances (the ‘reflected banana’ and ‘reflected fish’ families) make their appearance. The lower two panels show the partial integral is poorly conserved for these families. Near the thin-tube orbit, though, the conservation is good.

0.9, $E = -5.5811$). The upper and lower panels show the (R, p_R) and (R, p_z) cross-sections at the equator for large and small L_z respectively. In each case, the orbits are marked with the percentage fluctuation of the partial integral. At high L_z , there is the reassuring picture of good conservation of the partial integral all across the surface of section. The orbits are all tubes. At low L_z , the resonances associated with the ‘reflected banana’ and ‘reflected fish’ families (see e.g. Lees & Schwarzschild 1992; E94) make their appearance. The partial integral is poorly conserved on the islands in the lower panels of Fig. 7. Only near the thin-tube orbits and near the orbits confined to the equatorial plane is the preservation of the partial integral at all good in the lower-panels. It is useful to contrast this behaviour with that of the classical integral L^2 , which does not distinguish between any of the orbits on the lower panel of Fig. 7. We conclude then that I_3 is a useful discriminant between orbits of the same E and L_z .

Although we have only presented numerical evidence for the power-law models, which have spheroidal equipotentials, nonetheless the derivation given in Section 4.1 suggests that our partial integral is good for thin and near-thin tubes in all axisymmetric scale-free potentials. It would be interesting to substantiate this claim for other scale-free galaxy models – such as those studied by Toomre (1982) for instance.

5 THREE-INTEGRAL DISTRIBUTION FUNCTIONS

We now exploit the partial integral for the scale-free power-law models to build simple three-integral DFs by superposing basic component solutions of the collisionless Boltzmann equation. First, we develop some preliminary results concerning our components in Section 5.1. Then, in the next section, we pass to the actual construction of the approximate analytical three-integral DFs by superposition of the components.

5.1 Components

The two exact integrals $I_1 = |E|$, $I_2 = L_z^2$ and the partial integral I_3 can be used to construct component DFs $f(I_1, I_2, I_3)$. Let us note that all such DFs correspond to spherically aligned Jeans solutions, i.e.,

$$\langle v_r v_\theta \rangle = \langle v_\theta v_\phi \rangle = \langle v_r v_\phi \rangle \equiv 0. \quad (5.1)$$

This general result follows directly from the forms of the integrals. In particular, it depends on the absence of velocity cross-terms in the partial integral. Is it possible to improve the accuracy of the partial integral by incorporating velocity cross-terms, which generate misalignment of the velocity ellipsoid with the spherical polar coordinates? We have explored this question with numerical orbit integration. It appears that some slight improvement of the partial integral is possible, but only at the cost of increasing mathematical complexity of the partial integral. We believe that the coefficient of any cross-term must be small, and so any misalignment of the stresses from spherical polars is also limited.

To build three-integral DFs, we shall find it useful to study the properties of two sets of components. The first set is just the product of powers of the integrals (cf., Fricke 1951; White 1985; ZES)

$$f_{k,n,m} = I_1^k I_2^n I_3^m. \quad (5.2)$$

The density generated by (5.2) is

$$\rho_{k,n,m} \propto \frac{r^{(2-\beta)(m+n)-\beta(k+3/2)} \sin^{2n} \theta [g(\theta)]^m}{[g(\theta)]^{\beta(k+m+n)/2+3\beta/4}}. \quad (5.3)$$

To reproduce the r -dependence of the density, we must have

$$k = \frac{(2-\beta)(m+n)}{\beta} + \frac{2}{\beta} - \frac{1}{2}, \quad (5.4)$$

so that (5.3) simplifies to

$$\rho_{n,m} = \frac{S_{n,m}}{r^{2+\beta}} \frac{\sin^{2n} \theta}{[g(\theta)]^{1+n+\beta/2}}, \quad (5.5)$$

with

$$S_{m,n} = \frac{\sqrt{\pi} 2^{m+n+3/2} \Gamma(m+n+1) B(1/2, n+1/2)}{|\beta|^{1+2(m+n+1)/\beta}} \times \begin{cases} \frac{\Gamma(-1-2(m+n+1)/\beta)}{\Gamma(1/2-2/\beta-(2-\beta)(m+n)/\beta)}, & \text{if } \beta < 0, \\ \frac{\Gamma(1/2+2/\beta+(2-\beta)(m+n)/\beta)}{\Gamma(2+2(m+n+1)/\beta)}, & \text{if } \beta > 0. \end{cases} \quad (5.6)$$

The second set of components is

$$g_{k,n,m} = I_1^k I_2^n (I_3 + C I_2)^m. \quad (5.7)$$

Here, C is a constant, which we assume to be small and check a posteriori. Again, to reproduce the r -dependence of the density, k is restricted to (5.4). The density corresponding to (5.7) is

$$\rho_{n,m} = \frac{S_{n,m}}{r^{2+\beta}} \frac{\sin^{2n} \theta}{[g(\theta)]^{1+n+\beta/2}} \left[1 + C \frac{m(2n+1)}{2(n+1)} \frac{\sin^2(\theta)}{g(\theta)} \right]. \quad (5.8)$$

This follows on taking the Taylor expansion of (5.7) and then using (5.5) twice. In the spherical limit, we shall show that $C = 0$. Therefore, both sets of components (5.2) and (5.7) are axisymmetric generalisations of the components (3.4) in the spherical limit.

5.2 5.2 Three-Integral DFs

DFs that can reproduce the power-law density are given by restricting attention to just the $n = 0$ and $n = 1$ components in (5.5) and (5.8). We choose to investigate DFs of the form:

$$\begin{aligned} f &= \sum_m A_{0,m} g_{k,0,m} + A_{1,m} f_{k,1,m}, \\ &= \sum_m A_{0,m} I_1^{2/\beta+(2-\beta)m/\beta-1/2} (I_3 + CI_2)^m \\ &+ \sum_m A_{1,m} I_1^{2/\beta+(2-\beta)(m+1)/\beta-1/2} I_2 I_3^m, \end{aligned} \quad (5.9)$$

where the $A_{0,m}$ and $A_{1,m}$ are unknown amplitudes. This generates the density

$$\begin{aligned} \rho &= \frac{1}{r^{2+\beta} g^{2+\beta/2}(\theta)} \left[g(\theta) \sum_m A_{0,m} S_{0,m} \right. \\ &\left. + \sin^2 \theta \left(\sum_m \frac{1}{2} m C A_{0,m} S_{0,m} + A_{1,m} S_{1,m} \right) \right]. \end{aligned} \quad (5.10)$$

If the DF only depends on globally defined classical integrals, then it obviously satisfies the Jeans equations. This is not guaranteed for DFs depending on any partial or approximate integrals. So, we must also compare the kinematics of the DFs (5.9) with the solutions of the Jeans equation derived earlier in Section 2. By straightforward integration over velocity space, we discover that the DFs (5.9) generate the second moments:

$$\begin{aligned} \rho \langle v_r^2 \rangle &= \frac{1}{r^{2+2\beta} g^{2+\beta}(\theta)} \left[\frac{1}{2} g(\theta) \sum_m \frac{A_{0,m} S_{0,m}}{(1+m+\beta)} \right. \\ &\left. + \frac{1}{2} \sin^2 \theta \sum_m \frac{A_{1,m} S_{1,m}}{(2+m+\beta)} \right], \\ \rho \langle v_\theta^2 \rangle &= \frac{1}{r^{2+2\beta} g^{2+\beta}(\theta)} \left[\frac{1}{2} g(\theta) \sum_m \frac{(1+m) A_{0,m} S_{0,m}}{(1+m+\beta)} \right. \\ &- \frac{1}{8} C \sin^2 \theta \sum_m \frac{m(1+m) A_{0,m} S_{0,m}}{(1+m+\beta)} \\ &\left. + \frac{1}{4} \sin^2 \theta \sum_m \frac{(2+m) A_{1,m} S_{1,m}}{(2+m+\beta)} \right], \\ \rho \langle v_\phi^2 \rangle &= \frac{1}{r^{2+2\beta} g^{2+\beta}} \left[\frac{1}{2} g(\theta) \sum_m \frac{(1+m) A_{0,m} S_{0,m}}{(1+m+\beta)} \right. \\ &+ \frac{1}{4} C \sin^2 \theta \sum_m \frac{m(1+m) A_{0,m} S_{0,m}}{(1+m+\beta)} \\ &\left. + \frac{3}{4} \sin^2 \theta \sum_m \frac{(2+m) A_{1,m} S_{1,m}}{(2+m+\beta)} \right]. \end{aligned} \quad (5.11)$$

As expected, this is a spherically aligned solution and all the cross-terms of the velocity dispersion tensor vanish.

Now, the density of the scale-free power-law models can be expanded as:

$$\begin{aligned} \rho &= \frac{1}{r^{2+\beta} g^{2+\beta/2}(\theta)} \left[(2 - Q(1 + \beta)) g(\theta) \right. \\ &\left. + (\beta + 2)(Q - 1) \sin^2 \theta \right]. \end{aligned} \quad (5.12)$$

The spherically aligned Jeans solution can be deduced from (2.20) by putting $H_2 = 0$. We obtain:

$$\begin{aligned} \rho \langle v_r^2 \rangle &= \frac{(1 + \beta)^{-1}}{r^{2+2\beta} g^{2+\beta}(\theta)} \left[\left[\frac{1}{2} (2 - Q(1 + \beta)) + H_1 q^2 \right] g(\theta) \right. \\ &\left. + (Q - 1)(1 + \beta) \left(\frac{1}{2} + H_1 q^2 \right) \sin^2 \theta \right], \\ \rho \langle v_\theta^2 \rangle &= \frac{(1 + \beta)^{-1}}{r^{2+2\beta} g^{2+\beta}(\theta)} \left[\left[\frac{1}{2} (2 - Q(1 + \beta)) - \beta q^2 H_1 \right] g(\theta) \right. \\ &\left. + \frac{1}{2} (Q - 1)(1 + \beta) \sin^2 \theta \right], \\ \rho \langle v_\phi^2 \rangle &= \frac{(1 + \beta)^{-1}}{r^{2+2\beta} g^{2+\beta}(\theta)} \left[\left[\frac{1}{2} (2 - Q(1 + \beta)) - \beta q^2 H_1 \right] g(\theta) \right. \\ &\left. + (Q - 1)(1 + \beta) \left(\frac{3}{2} - 2\beta q^2 H_1 \right) \sin^2 \theta \right]. \end{aligned} \quad (5.13)$$

We must now choose the amplitudes $A_{0,m}$ and $A_{1,m}$ and the constant C so that the densities (5.10) and (5.12) and the kinematics (5.11) and (5.13) coincide. The calculation is straightforward and reveals that

$$C = -\frac{6}{5}(Q - 1). \quad (5.14)$$

This verifies that C is small, at least for moderate flattenings. This justifies the first-order Taylor expansions used in our analysis. For example, if the flattening is E3, then $q \sim 0.9$, and so the next term in the Taylor expansion is $O(C^2)$ which is $\sim 8\%$. The constraints concerning the unknown amplitudes $A_{0,m}$ and $A_{1,m}$ are most compactly written by introducing the weights

$$\begin{aligned} A_{0,m} S_{0,m} &= (2 - Q(1 + \beta)) W_{0,m}, \\ A_{1,m} S_{1,m} &= (\beta + 2)(Q - 1) W_{1,m}. \end{aligned} \quad (5.15)$$

Then, there are three conditions on the $W_{0,m}$, namely

$$\begin{aligned} \sum_m W_{0,m} &= 1, \\ \sum_m \frac{W_{0,m}}{1+m+\beta} &= \frac{1}{1+\beta} + \frac{2q^2 H_1}{(1+\beta)(2-Q(1+\beta))}, \\ \sum_m m W_{0,m} &= \frac{2\beta q^2 H_1}{3[2-Q(1+\beta)]}. \end{aligned} \quad (5.16)$$

There are two conditions on the $W_{1,m}$, namely

$$\begin{aligned} \sum_m W_{1,m} &= 1 + \frac{2\beta}{5(\beta+2)} q^2 H_1, \\ \sum_m \frac{W_{1,m}}{2+m+\beta} &= \frac{1+2q^2 H_1}{2+\beta}. \end{aligned} \quad (5.17)$$

Provided we choose at least three of the weights $W_{0,m}$ and at least two of the weights $W_{1,m}$, these linear equations (5.16) and (5.17) can always be solved. Of course, it is not

guaranteed that the DFs formed by superposing the components are positive definite. This is a hard matter to check analytically, but easy to do on a finite grid with the computer. In practice, we did not find positivity to be a real constraint here. We have verified numerically that some of the DFs for the model with $\beta = 0.18, q = 0.9$ are indeed positive definite. In particular, we examined the four cases $H_1 = \pm 0.1$ and ± 0.3 , with the non-vanishing weights chosen as $W_{0,0}, W_{0,10}, W_{0,20}, W_{1,0}$ and $W_{1,20}$. It seems that, at least for moderate flattenings and anisotropies, many of the three-integral DFs constructed according to this recipe are everywhere positive in phase space.

The DFs (5.9) therefore seem to show that the spherically aligned Jeans solutions ($H_2 = 0$), which are marked by the bold lines in Figs. 1 and 2, are physical. This conclusion certainly holds good for tangentially anisotropic solutions with $H_1 \lesssim 0$. When H_1 becomes large and positive, the stress tensor is radially distended. This is caused by the presence of eccentric radial orbits in the model, for which our partial integral is not a good invariant. In this limit, it is unwise to put undue faith in our DF. In the spherical limit, $C = W_{1,m} = A_{1,m} = 0$. This means that the second sum in (5.9) vanishes. The partial integral I_3 reduces to L^2 and so we recover the DFs given in Section 3 of this paper, as we should.

There is one further, somewhat special, limit that deserves mention. When $\beta = 2$, the scale-free power-law potential is not useful for modelling galaxies, as it generates negative density through Poisson's equation. Nonetheless, it is perfectly reasonable to consider the properties of orbits in this supplied force field. The case is exceptional because the Hamilton-Jacobi equation separates (e.g., Landau & Lifshitz 1960; Lynden-Bell 1962). So, in this limit, there is an exact, global third integral of the form

$$I_{3,g} = \frac{1}{2} \left[r^2 (v_\theta^2 + v_\phi^2) - \frac{1}{g(\theta)} \right]. \quad (5.18)$$

Now, our partial integral (4.9) does not reduce to this global integral when $\beta = 2$. This, however, is no problem. Any thin tube, which is a one-dimensional manifold, must possess conserved quantities additional to the globally defined integrals. The partial integral valid for thin tubes (4.9) need not therefore reduce to (5.18). When $\beta = 2$, we see that

$$I_3 = 2I_{3,g}g(\theta) + 1. \quad (5.19)$$

Any change in the partial integral ΔI_3 therefore satisfies

$$\Delta I_3 = 2I_{3,g}\Delta g(\theta), \quad (5.20)$$

We see that this change must be small for the thin tubes, because $I_{3,g} \approx 0$ from (4.6). Note, too, that it follows from the form of (5.18) that the velocity ellipsoid is spherically aligned when $\beta = 2$ (in fact, this is a special case of Eddington's (1915) theorem). It is interesting that this somewhat exceptional case seems to reinforce our arguments for the physical nature of the spherically aligned Jeans solutions.

6 6 CONCLUSIONS

One way forward in the construction of three-integral galaxy models is to exploit partial integrals. These are invariants of the motion specific to particular orbital families. Phase

space is therefore broken up into patches, and each patch is covered by an appropriate integral. This general picture is similar to that advocated by Binney and co-workers (e.g., Binney 1994; Kaasalainen & Binney 1994), who fit phase space tori to different orbital families using different mappings. It also has some tradition in the theory of resonant orbits (Gerhard & Saha 1991; Dehnen & Gerhard 1993). The main result of this paper is the identification of such a partial integral for the thin and near-thin tubes in arbitrary axisymmetric scale-free potentials. It is a generalisation of the total angular momentum. By careful numerical orbit integration, the excellence of the partial integral for the thin tubes in one family of models – the scale-free power-law models (E94) – has been verified in detail. This supplements earlier work on the scale-free logarithmic potential (ZES). For all the orbits we have examined in flattened potentials, this partial integral is *always* better conserved than the total angular momentum

Approximate and partial integrals are needed in stellar dynamics for the construction of distribution functions (DFs). For the particular case of the scale-free power-law models, we carried out a detailed analysis of how to build three-integral DFs. This yielded the following conclusions:

- (1) If DFs depend on any approximate or partial integral, it is not guaranteed that they satisfy the Jeans equations. To be sure of building a galaxy model in which the motions of the stars balance the force field, it is important to combine both the Jeans and Boltzmann approaches. We have shown, both here and in ZES, that such combined Jeans and Boltzmann solutions can be found in a simple way.
- (2) The solution of the Jeans equations for arbitrary axisymmetric scale-free models has been deduced. Jeans solutions in which the velocity ellipsoid is spherically aligned probably are physical, at least for moderate flattenings and anisotropies. This holds because the partial integral is quadratic in the velocities and does not generate any cross-terms in the stress tensor. At present, it is not known whether any of the remaining Jeans solutions are physical. Even at the level of the Jeans equations, it is evident that we cannot construct very radially anisotropic models with strong cusps ($\beta > 0$).
- (3) DFs depending on the classical integrals E and L_z and the partial integral for near-thin tubes I_3 can generate both the density and the spherically-aligned second moments of the power-law models. The scale-free power-law models are now a simple and useful set of galaxy models which have both two-integral and three-integral DFs readily available.

There are three pressing questions left unresolved by the work in ZES and this paper. First, what is the appropriate partial integral to choose for the radial orbits in scale-free models? Although the phase space areas occupied by the thin and near-thin tubes are patched by the partial integral deduced here, the areas occupied by the eccentric radial orbits are not. The answer to this question is needed to build radially anisotropic three-integral DFs. Second, although one sub-set of the Jeans solutions displayed in Figs. 1 and 2 has been shown to be physical by construction of suitable DFs, the status of the remaining solutions is unclear. Is it possible that at least some – perhaps even all – of the remaining Jeans solutions are physically realisable? This is,

of course, related to the first question, as the Jeans solutions must be built by DFs depending on partial integrals appropriate to other orbital families. Third, how does this work generalise to fully triaxial scale-free models? Here, the solutions of the Jeans equations are now explicitly available (Carollo, de Zeeuw & Evans 1996), but there are no known integrals other than energy.

ACKNOWLEDGMENTS

NWE thanks the Royal Society for financial support. RMH is partially supported by the Particle Physics and Astronomy Research Council. PTdZ thanks Theoretical Physics, Oxford for their hospitality during a working visit. We wish to thank Ortwin Gerhard for some perceptive comments on scale-free models, as well as Massimo Stiavelli, Jos de Bruijne and an anonymous referee for helpful criticism of the draft manuscript.

REFERENCES

- Arnold R., 1992, MNRAS, 257, 225
 Bacon R., 1985, A&A, 143, 84
 Binney J. J., 1981, MNRAS, 196, 455
 Binney J. J., 1994, in Morrison L. V., Gilmore G., eds, Galactic and Solar System Optical Astrometry. Cambridge Univ. Press, Cambridge, p. 141
 Binney J. J., Davies R. L., Illingworth G. D., 1991, ApJ, 361, 78
 Binney J. J., Tremaine S. D., 1987, Galactic Dynamics. Princeton University Press, Princeton
 Carollo M., de Zeeuw P. T., Evans N. W., 1996, MNRAS, submitted
 Casertano S., van Gorkom J., 1991, AJ, 101, 1231
 de Bruijne J. H. J., van der Marel R. P., de Zeeuw P. T., 1996, MNRAS, 282, 909
 Dehnen W., Gerhard O.E., 1993, MNRAS, 261, 311
 Dejonghe H., de Zeeuw P. T., 1988, ApJ, 333, 90
 de Zeeuw P. T., 1985, MNRAS, 216, 273
 de Zeeuw P. T., Evans N. W., Schwarzschild M., 1996, MNRAS, 280, 903 (ZES)
 de Zeeuw P. T., Lynden-Bell D., 1985, MNRAS, 215, 713
 Eddington A. S., 1915, MNRAS, 76, 37
 Evans N. W., 1990, Phys. Rev. A, 41, 5666
 Evans N. W., 1994, MNRAS, 267, 333 (E94)
 Evans N. W., de Zeeuw P. T., 1994, MNRAS, 271, 202
 Fricke W., 1951, Astron. Nach., 280, 193
 Gerhard O. E., 1991, MNRAS, 250, 812
 Gerhard O. E., Saha P., 1991, MNRAS, 251, 449
 Gutzwiller M. C., 1990, Chaos in Classical and Quantum Mechanics. Springer-Verlag, Berlin
 Hunter C., 1977, AJ, 82, 271
 Innanen K. P., Papp K. A., 1977 AJ, 82, 322
 Kaasalainen M., Binney J. J., 1994, MNRAS, 268, 1033
 Kulsaa A. S., Lynden-Bell D., 1992, MNRAS, 255, 105
 Landau L., Lifshitz E.M., 1960, Mechanics. Pergamon Press, Oxford, p. 149
 Lees J., Schwarzschild M., 1992, ApJ, 384, 491
 Lupton R., Gunn J., 1987, AJ, 93, 1106
 Lynden-Bell D., 1962, MNRAS, 124, 95
 Maoz E., Bekenstein J., 1990, ApJ, 353, 59
 Mathews J., Walker R., 1964, Mathematical Methods of Physics. Benjamin, California, Chapter 4
 Mathieu A., Dejonghe H., Hui X., 1996, A&A, 309, 30
 Merritt D., 1985, AJ, 90, 1027
 Morrison H., Flynn B., Freeman K., 1990, AJ, 100, 1191
 Norris J., 1986, ApJS, 61, 667
 Osipkov L. P., 1979, Pis'ma Astr. Zh., 5, 77
 Richstone D. O., 1980, ApJ, 238, 103
 Saaf A., 1968, ApJ, 154, 483
 Schwarzschild M., 1979, ApJ, 232, 236
 Toomre A., 1982, ApJ, 259, 535
 van der Marel R. P., 1991, MNRAS, 253, 710
 White S. D. M., 1985, ApJ, 294, L99

7 APPENDIX A: JEANS SOLUTIONS FOR CORED MODELS

Here, we give the extension of solution (2.20) to the stresses associated with slightly more general axisymmetric densities in the potentials of the cored power-law models (E94).

We consider the general density law:

$$\rho = \frac{a_1 R^2 + c_1 z^2 + d_1 R_c^2}{(R_c^2 + R^2 + z^2/q^2)^{1+\gamma/2}}, \quad (\text{A1})$$

with a_1 , c_1 , d_1 and γ free parameters. The potential is

$$\Phi = \begin{cases} \frac{1}{2} \ln(R_c^2 + R^2 + z^2/q^2), & \text{for } \beta = 0, \\ -\frac{R_c^\beta}{\beta(R_c^2 + R^2 + z^2/q^2)^{\beta/2}}, & \text{for } \beta \neq 0. \end{cases} \quad (\text{A2})$$

Here, R_c is the core radius. When $R_c = 0$ we recover the scale-free potentials (2.1) with $g(\theta)$ given in (2.4). The two-parameter solution of the Jeans equations is:

$$\begin{aligned} \rho \langle v_R^2 \rangle &= \frac{1}{(\alpha-1)} \frac{A_1 R^2 + C_1 z^2 + D_1 R_c^2}{(R^2 + z^2/q^2 + R_c^2)^\alpha}, \\ \rho \langle v_R v_z \rangle &= \frac{1}{(\alpha-1)} \frac{B_2 R z}{(R^2 + z^2/q^2 + R_c^2)^\alpha}, \\ \rho \langle v_z^2 \rangle &= \frac{1}{(\alpha-1)} \frac{A_3 R^2 + C_3 z^2 + D_3 R_c^2}{(R^2 + z^2/q^2 + R_c^2)^\alpha}, \\ \rho \langle v_\phi^2 \rangle &= \frac{1}{(\alpha-1)} \frac{A_4 R^2 + C_1 z^2 + D_1 R_c^2}{(R^2 + z^2/q^2 + R_c^2)^\alpha}. \end{aligned} \quad (\text{A3})$$

Here, $\alpha = (2 + \gamma + \beta)/2$ and the relationships between the coefficients and the H_1 and H_2 parameters are given in Table 4.

Self-consistent models have

$$\begin{aligned} a_1 &= \frac{1}{q^2} (1 - \beta q^2), \\ c_1 &= \frac{1}{q^2} \left(2 - \frac{1 + \beta}{q^2} \right), \\ d_1 &= \frac{1}{q^2} + 2, \\ \gamma &= \alpha + 2 + \beta. \end{aligned} \quad (\text{A4})$$

Upon substitution of these expressions, and taking the limit $R_c = 0$, we recover the results in Section 2.4 of the main text.

It is instructive to transform to spheroidal coordinates (λ, ϕ, ν) , with (λ, ν) the two roots for τ of $R^2/(\tau - R_c^2) + z^2/(\tau - q^2 R_c^2) = 1$. The foci lie at $(R = 0, z = \pm R_c \sqrt{1 - q^2})$, and λ and ν are given by

$$\begin{aligned} \lambda, \nu &= \frac{1}{2} [R^2 + z^2 + R_c^2 (1 + q^2)] \pm \\ &\frac{1}{2} \sqrt{(R^2 + z^2)^2 + 2R_c^2 (1 - q^2) (R^2 - z^2) + R_c^4 (1 - q^2)^2}. \end{aligned} \quad (\text{A5})$$

Table 4. Coefficients for the Jeans solution (A3).

A_1	$[(\alpha-1)+(2-\alpha)q^2]H_1+(\alpha-1)H_2$ $+\frac{(\alpha-1)a_1+q^2c_1}{2\alpha}$
C_1	$(2-\alpha)H_1+\frac{(\alpha-1)}{q^2}H_2+\frac{1}{2}c_1$
D_1	$[(\alpha-1)+(2-\alpha)q^2]H_1$ $+(\alpha-1)H_2+\frac{q^2c_1+(\alpha-1)d_1}{2\alpha}$
B_2	$(\alpha-1)H_1$
A_3	$(2-\alpha)q^2H_1+\frac{(\alpha-1)a_1+q^2c_1}{2\alpha}$
C_3	$H_1+\frac{1}{2}c_1$
A_4	$(2-\alpha)[2\alpha-2+(3-2\alpha)q^2]H_1$ $+(\alpha-1)(3-2\alpha)H_2+\frac{3(\alpha-1)a_1+(3-2\alpha)q^2c_1}{2\alpha}$

The potential then simplifies to

$$\Phi = \begin{cases} \frac{1}{2} \ln \lambda + \frac{1}{2} \ln \nu + \ln q R_c, & \text{for } \beta = 0, \\ -\frac{1}{\beta} \left(\frac{R_c^4 q^2}{\lambda \nu} \right)^{\beta/2}, & \text{for } \beta \neq 0. \end{cases} \quad (\text{A6})$$

The Jeans solutions (A3) can be rewritten to give $\rho(v_\lambda^2)$, $\rho(v_\lambda v_\nu)$, and $\rho(v_\nu^2)$ by means of the relations between (v_R, v_z) and (v_λ, v_ν) given in, e.g., Dejonghe & de Zeeuw (1988). In particular, we find

$$(\lambda - \nu)\rho(v_\lambda v_\nu) = -\frac{H_2 R z}{(R_c^2 + R^2 + z^2/q^2)^{\alpha-1}}. \quad (\text{A7})$$

This allows us to consider three limiting cases at once.

When $q = 1$ the potential – but not necessarily the density – is spherical. The foci of the spheroidal coordinates now coincide with the origin, and hence (λ, ϕ, ν) reduce to ordinary spherical coordinates, with $v_\lambda = v_r$ and $v_\nu = -v_\theta$. It follows that $\langle v_r v_\theta \rangle \propto H_2$. But in a spherical potential this cross term in the stress tensor must vanish by the symmetries of the individual stellar orbits, so that the only Jeans solutions with physical DFs are those with $H_2 = 0$. This result is valid for arbitrary β and R_c .

When $\beta = 2$ the potential is of Stäckel form in the coordinates (λ, ϕ, ν) , for arbitrary q and R_c (de Zeeuw & Lynden-Bell 1985). It then admits three exact integrals of motion that are quadratic in the velocity components, and any DF will therefore give $\langle v_\lambda v_\nu \rangle \equiv 0$. In this limit we must therefore also restrict the Jeans solutions (A3) to those with $H_2 = 0$, irrespective of the values of q and R_c .

When $R_c = 0$ the spheroidal coordinates again reduce to sphericals, but the potential is flattened unless $q = 1$. In this case the model potential is scale-free, but there is no restriction on H_2 , unless $q = 1$ or $\beta = 2$.

The above shows that if we consider our Jeans solutions as functions of the parameters q and β , then along the two boundaries $q = 1$ and $\beta = 2$ of the parameter-space they must reduce to a one-parameter family, with $H_2 = 0$. There appears to be no physical reason for a similar restriction in the entire (q, β) -plane.

Finally, we remark that the line-of-sight projected second moments associated with the solutions (A3) are all of the general form (3.7) of Evans & de Zeeuw (1994), where

the coefficients a_{ij} , b_{ij} , c_{ij} and d_{ij} can be worked out explicitly.

8 APPENDIX B: CONSTRAINTS ON THE POSITIVITY OF THE PRINCIPAL STRESSES

In this appendix, we write out explicitly the constraint that the two-parameter Jeans solutions discussed in Sections 2.4 and 2.5 have positive principal components. The areas inside the following four curves must be deleted from Figs. 1 and 2.

$$H_2 = \frac{(1-Q)(Q^2-Q+\beta(Q^2+Q+2H_1))^2}{2Q(1+\beta)(2QH_1-Q(Q-1)^2+\beta(2H_1+Q-Q^3))}.$$

$$H_2 = \frac{(1-Q)(Q^2-2Q-H_1+\beta Q^2+\beta H_1)}{Q(1+\beta)} \times \frac{Q^2-Q+2\beta H_1+\beta Q(1+Q)}{Q(5Q-2Q^2+4H_1-3)-2H_1+\beta(2H_1+Q+Q^2-2Q^3)}.$$

$$H_2 = \frac{(1-Q)(Q+H_1Q+\beta(H_1Q-2H_1-Q))}{Q(1+\beta)} \times \frac{\beta(Q^2+Q+2H_1)-Q(1-Q)}{Q(2-2H_1-3Q+Q^2)+\beta(Q^3+Q^2+2H_1Q-2Q-4H_1)}.$$

$$H_2 = \frac{H_1(1-Q)}{Q(1+\beta)(2H_1+Q-Q^2)^2} \times \left[(Q(Q^3-2Q^2-Q-2H_1(1+Q))+\beta(Q^2+Q^4+4H_1^2+4QH_1)) \pm 2Q[(2H_1+Q)(Q-2\beta H_1-\beta Q)(2H_1+2Q-Q^2-\beta Q^2)]^{\frac{1}{2}} \right].$$

These lengthy expressions are readily evaluated numerically. A quick check on their accuracy is provided by taking the limit $\beta = 0$, when they reduce to equations (2.38) of ZES.

9 APPENDIX C: TRIAXIAL COMPONENTS WITH TRIAXIAL KINEMATICS

Almost certainly, the potentials of galaxy haloes are not exactly spherical. But, one of the very attractive reasons for using spherical potentials is the ready availability of four functionally-independent integrals of the motion E, L_x, L_y and L_z . As realised clearly by White (1985) and Arnold (1992), this is useful for building axisymmetric tracer populations with triaxial kinematics – as is warranted by the shape of the local velocity ellipsoid in the Milky Way, for example. The same methods can also be exploited to give *triaxial* tracer populations with triaxial kinematics! (c.f., Mathieu, Dejonghe & Hui 1996).

Together with White (1985), the work in Section 3 shows that the DFs

$$f_{m,n}(E, L^2, L_z^2) = \begin{cases} \eta_{m,n} L^{2m} L_z^{2n} |E|^\alpha, & \text{if } \beta \neq 0, \\ \eta_{m,n} L^{2m} L_z^{2n} \exp(-E), & \text{if } \beta = 0, \end{cases} \quad (\text{C1})$$

generate the density law

$$\rho = r^{-\gamma} \sin^{2n} \theta, \quad (\text{C2})$$

in the spherical scale-free power-law potentials

$$\Phi = \begin{cases} -\frac{1}{\beta r^\beta}, & \text{if } \beta \neq 0, \\ \log r, & \text{if } \beta = 0. \end{cases} \quad (\text{C3})$$

The constant $\eta_{m,n}$ is available as (3.7) when $\beta \neq 0$. For the logarithmic case ($\beta = 0$), ZES show that

$$\eta_{m,n} = \frac{(m+n+\frac{\gamma}{2})^{m+n+\frac{3}{2}}\Gamma(n+1)}{\pi\Gamma(n+\frac{1}{2})\Gamma(n+m+1)}. \quad (\text{C4})$$

But, there is nothing special about the z -axis, and no reason for the z -component of angular momentum to play a distinguished role! It is straightforward to show that the DFs

$$g_{m,n}(E, L^2, L_x^2) = \begin{cases} \eta_{m,n} L^{2m} L_x^{2n} |E|^\alpha, & \text{if } \beta \neq 0, \\ \eta_{m,n} L^{2m} L_x^{2n} \exp(-E), & \text{if } \beta = 0, \end{cases} \quad (\text{C5})$$

give the stellar density

$$\rho = r^{-\gamma} \left[\sin^2 \theta \sin^2 \phi + \cos^2 \theta \right]^n, \quad (\text{C6})$$

and the kinematics

$$\begin{aligned} \langle v_r^2 \rangle &= \frac{v_{\text{circ}}^2}{2m + 2n + \beta + \gamma}, \\ \langle v_\theta^2 \rangle &= \frac{m+n+1}{n+1} \frac{(2n+1) \sin^2 \phi + \cos^2 \theta \cos^2 \phi}{\sin^2 \phi + \cos^2 \theta \cos^2 \phi} \langle v_r^2 \rangle, \\ \langle v_\phi^2 \rangle &= \frac{m+n+1}{n+1} \frac{\sin^2 \phi + (2n+1) \cos^2 \theta \cos^2 \phi}{\sin^2 \phi + \cos^2 \theta \cos^2 \phi} \langle v_r^2 \rangle, \\ \langle v_\theta v_\phi \rangle &= \frac{n(m+n+1)}{n+1} \frac{\sin \phi \cos \phi \cos \theta}{\sin^2 \phi + \cos^2 \theta \cos^2 \phi} \langle v_r^2 \rangle. \end{aligned} \quad (\text{C7})$$

Equally, the DFs

$$h_{m,n}(E, L^2, L_y^2) = \begin{cases} \eta_{m,n} L^{2m} L_y^{2n} |E|^\alpha, & \text{if } \beta \neq 0, \\ \eta_{m,n} L^{2m} L_y^{2n} \exp(-E), & \text{if } \beta = 0, \end{cases} \quad (\text{C8})$$

correspond to

$$\rho = r^{-\gamma} \left[\sin^2 \theta \cos^2 \phi + \cos^2 \theta \right]^n, \quad (\text{C9})$$

with the kinematics (C7) on making the modifications $\cos \phi \rightarrow \sin \phi$ and $\sin \phi \rightarrow -\cos \phi$. Using the method of superposition of components, a very general DF corresponding to a triaxial halo with a triaxial velocity ellipsoid is

$$\begin{aligned} f(E, L_x^2, L_y^2, L_z^2) &= \sum_{m,n} A_{m,n} f_{m,n}(E, L^2, L_z^2) \\ &+ \sum_{m,n} B_{m,n} g_{m,n}(E, L^2, L_x^2) \\ &+ \sum_{m,n} C_{m,n} h_{m,n}(E, L^2, L_y^2). \end{aligned} \quad (\text{C10})$$

The components can find a ready application for fitting the data on the kinematics of the stellar halo of the Milky Way.

This paper has been produced using the Royal Astronomical Society/Blackwell Science \TeX macros.